Experimental Eye Research 174 (2018) 29–39

Contents lists available at ScienceDirect

Experimental Eye Research

journal homepage: www.elsevier.com/locate/yexer

Alpha-1-antitrypsin ameliorates inflammation and neurodegeneration in the diabetic mouse retina

Gustavo Ortiz[a], Emiliano S. Lopez[a], Juan P. Salica[a], Constanza Potilinski[a], Mariano Fernández Acquier[b], Eduardo Chuluyan[c], Juan E. Gallo[a,*]

[a] Nanomedicine & Vision Group, Facultad de Ciencias Biomédicas, Instituto de Investigaciones en Medicina Traslacional, Universidad Austral, Consejo Nacional de Investigaciones en Ciencia y Tecnología (CONICET), Avenida Presidente Perón 1500, Pilar, Buenos Aires, Argentina
[b] Servicio de Neumonología, Hospital Cetrángolo, Italia 1750, Vicente López, Buenos Aires, Argentina
[c] Centro de Estudios Farmacológicos y Botánicos, Paraguay 2155, Facultad de Medicina, Universidad de Buenos Aires, Buenos Aires, Argentina

ARTICLE INFO

Keywords:
Diabetes
Retina
Alpha 1-antitrypsin
Inflammation
Diabetic retinopathy
Blindness

ABSTRACT

Diabetic retinopathy (DR) is the most common cause of blindness in the working age population. Early events of DR are accompanied by neurodegeneration of the inner retina resulting in ganglion cell loss. These findings together with reduced retinal thickness are observed within the first weeks of experimental DR. Besides, an inflammatory process is triggered in DR in which the innate immune response plays a relevant role. Alpha 1 antitrypsin (AAT), an inhibitor of serine proteases, has shown anti-inflammatory properties in several diseases. We aimed at evaluating the use of AAT to prevent the early changes induced by DR. Diabetic AAT-treated mice showed a delay on ganglion cell loss and retinal thinning. These animals showed a markedly reduced inflammatory status. AAT was able to preserve systemic and retinal TNF-α level similar to that of control mice. Furthermore, retinal macrophages found in the AAT-treated diabetic mouse exhibited M2 profile ($F4/80^{+}CD206^{+}$) together with an anti-inflammatory microenvironment. We thus demonstrated that AAT-treated mice show less retinal neurodegenerative changes and have reduced levels of systemic and retinal TNF-α. Our results contribute to shed light on the use of AAT as a possible therapeutic option in DR.

1. Introduction

Diabetic retinopathy (DR) is the leading cause of blindness in the working age population (Lee et al., 2015) and is characterized by retinal changes that include microaneurisms, hemorrhages, hard and cotton-wool exudates, edema, neovessels and retinal detachment. According to these findings, DR is classified as non-proliferative, pre-proliferative and proliferative DR. Also retinopathy could be graded into mild, moderate or severe depending on the development of the disease. DR is characterized by a slow progression that usually takes several years to reach the advanced stages (Viswanath and McGavin, 2003).

In the diabetic patient the retinal neurovascular unit is affected by persistent hyperglycemia which generates degenerative changes and a chronic pro-inflammatory state (Antonetti et al., 2012). Both processes are responsible for early changes in the retina and involve different types of cells such as endothelial cells, pericytes, Müller cells, microglia, ganglion cells and bone marrow (BM) derived cells (Tang and Kern, 2011; Abcouwer and Antonetti, 2013). Migration, homing and vascular reparative properties of BM-derived cells are affected in diabetes (Chakravarthy et al., 2016). In fact, trafficking of BM-derived monocytes/macrophages in the diabetic mouse retina (Rangasamy et al., 2014) and in patients with DR have been reported (Zeng et al., 2008). These cells are able to secrete inflammatory cytokines and chemokines as Interleukin-1-beta (IL-1β), Tumor Necrosis Factor Alpha (TNF-α) and interleukin-3 (IL-3) which have been found increased in the retina of diabetic animals (Hazra et al., 2013) and in the vitreous of patients with DR (Kocak et al., 2010). The role of TNF-α is well known in the development of diabetic retinopathy (Doganay et al., 2002; Joussen et al., 2002; Demircan et al., 2006).

It has been described that BM-derived macrophages are capable of developing into at least two main profiles: inflammatory M1 macrophages and anti-inflammatory M2 macrophages (Martinez and Gordon, 2014). The M1 profile is directly related to the expression and activity of the inducible nitric oxide synthase (iNOS) enzyme and the production of inflammatory cytokines such as TNF-α and IL-1β, as well as chemokines such as Monocyte Chemoatractant Protein 1 (MCP-1). The M1 type also presents $F4/80^{high}$ surface expression. The M2

* Corresponding author. Instituto de Investigaciones en Medicina Traslacional (CONICET – Universidad Austral), Av. Juan Perón 1500, Pilar, Buenos Aires, Argentina.
E-mail addresses: gaodelacalle@gmail.com (G. Ortiz), emilianoslopez@gmail.com (E.S. Lopez), jp.salica@gmail.com (J.P. Salica), constanza.potilinski@gmail.com (C. Potilinski), acquier@hotmail.com (M. Fernández Acquier), echuluyan@gmail.com (E. Chuluyan), jgallo06@gmail.com, jgallo@cas.austral.edu.ar (J.E. Gallo).

https://doi.org/10.1016/j.exer.2018.05.013
Received 27 February 2018; Received in revised form 2 May 2018; Accepted 14 May 2018
Available online 18 May 2018
0014-4835/

macrophages are related to the expression and activity of Arginase1 (Arg1) and present F4/80^{low} and the macrophage mannose receptor CD206^{high} expression in their surface (Porcheray et al., 2005; Martinez and Gordon, 2014). The M2 type is involved in the remodeling and repairing of different tissues as well as in the resolution of inflammatory processes (Bystrom et al., 2008; Laskin et al., 2011; Ortega-Gomez et al., 2013; Wynn et al., 2013). Although there is a large amount of data on how macrophages work in acute and chronic inflammation, their role in the development of DR has not been fully elucidated.

Alpha-1-antitrypsin (AAT) is an acute phase protein released mainly by hepatocytes during inflammation and acts as the major inhibitor of serine proteases (serpins) in blood (Lewis, 2012). Several researchers have pointed out the anti-inflammatory effects of AAT on the expression of neutrophil elastase (NE), cathepsin G and proteinase 3 by immune cells, as well as suppressing some cytokines and chemokines production, complement activation and immune cell infiltration (Gottlieb et al., 2014; Guttman et al., 2015). New evidence reveals that AAT has several mechanisms of action which do not involve serpin activity (Lewis, 2012; Jonigk et al., 2013). AAT is currently used in patients with deficit of AAT and non-genetic chronic obstructive pulmonary disease (Edgar et al., 2017). In this illness lung inflammation is driven by TNF-α (Cosio et al., 2009; Hurley et al., 2016).

Interestingly, investigations have found that AAT modulates lung inflammatory responses to TNF-α and suppress its production by stimulated macrophages (Churg et al., 2007; Jonigk et al., 2013). Also, serum levels of TNF-α were found reduced in AAT-treated diabetic mice accompanied by the fall of lymphocytic infiltration in a model of islet transplantation (Wang et al., 2017). As AAT modulates TNF-α, a major player in chronic inflammation and the pathogenesis of diabetic retinopathy, we thought it was interesting to evaluate the effect of AAT in experimental diabetic retinopathy. Furthermore, the modulation of pro-inflammatory factors represents an interesting approach to ameliorate the extent of damage caused by diabetes. This may enable prevention or delay in the development of diabetic complications such as DR. We expect that delivery of AAT affect and improve features of the pathology of diabetic retinopathy. The aim of our study was to evaluate the potential of AAT (Trypsan®, Grifolds, Barcelona, Spain) to moderate retinal degenerative and inflammatory changes that usually appear in the retina of diabetic mice (Yang et al., 2012). In order to achieve this, we evaluated the protein expression of several cytokines and chemokines, determined the level of TNF-alpha both in serum and retina, measured the thickness of the retina, counted retinal ganglion cells and made an analysis of the macrophage cells and its microenvironment in the retina.

2. Material and methods

2.1. Animals and model of diabetes

Eight-week-old male C57BL6J mice were purchased from Laboratory of Experimental Animals (LAE, Facultad de Ciencias Veterinarias, Universidad Nacional de La Plata, Buenos Aires). Animals were maintained at our Animal Resources Facilities (IIMT-CONICET) in accordance with the experimental ethical committee and the NIH guidelines on the ethical use of animals. The Animal Care Committee from School of Biomedical Sciences, Austral University, approved the experimental protocol (CICUAL IIMT 16–05). Model development was obtained as previously described (Li et al., 2010; Lai and Lo, 2013). Briefly, mice were intraperitoneally (i.p.) injected with 100 mg/kg streptozotocin (STZ) twice (day 0 and day 2). On day 9, a blood glucose test was performed on fasting 16 h. Animals with blood glucose levels of 200 mg/dl or higher were considered diabetic, and were used for the experimental groups (AAT-treated or untreated mice).

2.2. Cells

Raw 264.1 and J774.1 cells were maintained in RPMI supplemented with 10% heat-inactivated FBS (fetal bovine serum), 2 mmol/L L-glutamine, 100 U/mL streptomycin, and 100 mg/ml penicillin and incubated at 37 °C in a 5% CO_2 humidified atmosphere.

2.3. Glycemic levels, weight control, water consumption

C57BL6J mice were housed in groups (n = 7) with free access to food and water. Glycemic levels were evaluated fasting 16 h, taking one drop of blood from the tail vein and using test strips from One Touch Ultra kit (Johnson & Johnson, New Jersey, USA). Also, water consumption and weight were weekly monitored for 8 weeks until sacrifice (Supplementary material and Supplementary Fig. S1).

2.4. Human alpha-1-antitrypsin treatment

As previous studies described, animals were i.p. injected with 100 mg/kg AAT (2 mg/mouse) (Wang et al., 2017) in a 100 µl final volume, weekly during 8 weeks. In our laboratory we have indicated the presence of AAT in the microvasculature of the rat retina up to 6 days after intraperitoneal injection (Ortiz, 2013). Similar results were seen in mice.

2.5. Flatmount retinal ganglion cell quantification

Flatmount retinas were obtained as previously described (Gonzalez Fleitas et al., 2015), and incubated overnight with a polyclonal goat anti-Brn3a antibody (1:500; catalogue #: sc31984, Santa Cruz Biotechnology, CA, USA). After several washings, secondary antibodies were added, and sections were incubated for 2 h at room temperature. Images (200×; area corresponding to 0.1 mm^2) from 4 different quadrants from the central and peripheral retina were captured, and the mean of 20 images was considered as the representative value, and expressed as the total number of Brn3a(+) cells in 2 mm^2.

2.6. Measurement of retinal thickness

The eyes extracted were fixed in 4% paraformaldehyde (Sigma-Aldrich P-6148, USA) for 1 h. The anterior segment was dissected and removed as well as the vitreous and then the optic cup was left 16 h in fixation. Then, it was paraffin embedded. Five micron sections were performed. The histological sections were stained with hematoxylin and eosin for examination using the microscope Nikon Eclipse E800 (Tokyo, Japan). Thickness measurements in micrometers (µm) of different layers and the entire retina were quantified in the posterior retina from central (close to the optic disc) and peripheral retina. Image analyses were performed using a Nikon DXM1200 digital camera (Tokyo, Japan) mounted onto an Eclipse Nikon E−800 microscope for image acquisition. Images were digitalized in a rectangular frame of 1280 × 960 pixels using the 20 × objectives for thickness measurements. Statistical analysis was carried out using one-way analysis of variance.

2.7. ELISA for TNF-α

Serum samples of each animal at 8 week were taken. The four experimental groups (n = 4) were tested by ELISA using a specific kit to quantify TNF-α (DuoSet mouse TNF- α, cat#: DY493; R&D Systems, MN, USA) following the manufacturer's recommendations. Measures were done by triplicate. TNF-α level were determined using spectrophotometer and absorbance was measured at 450 nm with 540 nm correction according to the manufacturer's recommendations.

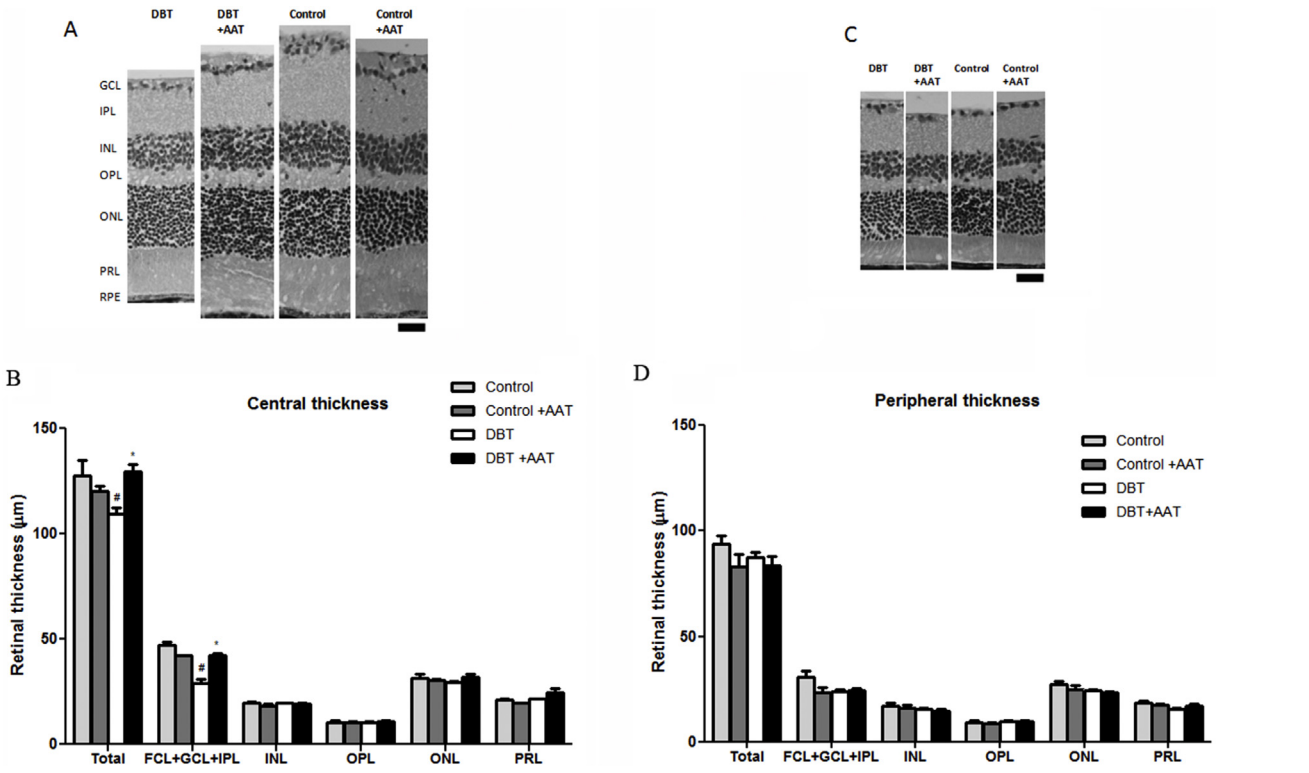

Fig. 1. (A) Representative photomicrographs stained with H&E show the histological appearance of central retinas from control (healthy mice), AAT-treated healthy mice (Control + AAT), untreated diabetic mice (DBT) and AAT-treated diabetic mice (DBT + AAT) at 8 weeks post diabetes induction. GCL: ganglion cell layer, IPL: inner plexiform layer; INL: inner nuclear layer, OPL: outer plexiform layer, ONL, outer nuclear layer, PRL: Photoreceptor Layer. RPE: Retinal Pigment Epithelium. (B) Quantification of central thickness. Differences in the Total layers, GCL and IPL were observed in control vs. DBT, and DBT vs. DBT + AAT groups (#$p < 0.05$ Control vs.DBT and *$p < 0.05$ DBT vs. DBT + AAT; Two way ANOVA; Bonferroni post-test). (C) Representative photomicrographs stained with H&E show the histological appearance of peripheral retinas from all experimental groups at 8 weeks. (D) Quantification of the total and different layers of peripheral thickness. No significant differences were observed in peripheral retina. Scale bar: 50 µm.

2.8. Reverse transcription-polymerase chain reaction (RT-PCR)

Total RNA from whole retina was extracted using Trizol Reagent (Sigma-Aldrich). Total RNA (1 µg) was reverse transcribed with 200 Units of Superscript II Reverse Transcriptase (Invitrogen) using 500 ng of Oligo (dT) primers. cDNAs were subjected to real-time polymerase chain reaction (qPCR) (Stratagene Mx3005p, Stratagene, La Jolla, CA). For qRT-PCR, the mRNA levels of *iNOS, arginase 1 (arg1) and f4/80*, were quantified by SYBR Green (Invitrogen, MA, USA), using the following primers: *iNOS* forward 5′- AAGATGGCCTGGAGGAATGC-3′and reverse 5′- TGCTGTGCTACAGTTCCGAG-3′; *arg1* forward 5′- CAGAAG AATGGAAGAGTCAG-3′ and reverse 5′- CAGATATGCAGGGAGTC ACC-3′; *f4/80* forward 5′- CTGTAACCGGATGGCAAACT -3′ reverse 5′- CTGTACCCACATGGCTGATG -3′.PCR amplifications were carried out using a cycle of 95 °C for 10 min and 40 cycles under the following parameters: 95 °C for 30 s, 56 °C for 30 s, 72 °C for 1 min. At the end of the PCR, the temperature was increased from 60 to 95 °C at a rate of 2 °C/minute, and fluorescence was measured every 15 s to construct the melting curve. Values were normalized to levels of glyceraldehyde-3-phosphate dehydrogenase transcript (*gapdh*; used as housekeeping) (forward 5′-ATCTCTGCCCCCTCTGCTG-3′and reverse 5′-GCCTGCTTCA CCACCTTCTTG-3′). Data were processed by the ΔΔCtmethod. The relative amount of the PCR product amplified from control AAT-untreated animals was set as 1. A non-template control (NTC) was run in every assay, and all determinations were performed as quadruplicates for each animal (n = 4/group) in three separated experiments.

2.9. Retina and serum cytokine proteome profiler array

Serum samples from each animal were taken at week 8 before sacrifice, used for a pool (n = 8). The proteome profiler mouse cytokine array panel A kit (cat #: ARY006, R&D Systems, MN, USA) was used to assess the levels of 40 cytokines in samples of interest. As detailed in the manufacturers' instructions, a single membrane with antibodies against 40 cytokines in duplicate spots was used per treatment group. Membranes were blocked with the supplied blocking buffer for 1 h and incubated with serum or retina samples pool of each experimental group overnight at 4 °C. Each serum pool was made up of 70 µl per animal. Briefly, the retina pool was performed as follows: seven retinas of each experimental group were extracted and incubated with RIPA buffer (150 mM sodium chloride 1.0%, Triton X-100 0.5%, sodium deoxycholate, 0.1% SDS, 50 mM Tris, pH 8.0) and protease inhibitor (Sigma Aldrich cat#: P8340). The extracts were lysed in rounds of frozen thawing at −80 °C and centrifuged at 15,000 rpm, keeping the supernatant ready to use. The spots were visualized using the enhanced chemiluminescence detection system (ECL, Amersham, Arlington Heights, IL, U.S.A.). Fluorescence intensity was measured using Image Studio Lite software (LI-COR, NE, USA). The average intensity of duplicate spots per antibody was calculated and plotted on a bar graph using Graph Pad Prism® 5.

2.10. Flow cytometry

At 8 weeks of AAT treatment, animals were anesthetized and eyes were extracted. Retinas were dissected and incubated with Hank's buffer and collagenase type I (Sigma Aldrich cat#: 9891) for 30 min at 37 °C. Single-cell suspension was prepared by mechanical disruption. Then, were stained with different conjugated-antibodies: anti-CD11b-APC (cat#: 553312; BD Biosciences) anti-F4/80-FITC (105155; Abcam, MA, USA), anti-CD206-PE (cat#: 553050; BD Biosciences), or isotypes

(rat IgG2bκ, ab1316125-rat monoclonal IgG2b, Rat IgG2a respectively) diluted in PBS 1% of BFS. For *in vitro* assay, 1×10^6 J774.1 or Raw264.1 cells were incubated with CD206-PE and F4/80-FITC antibodies or isotypes diluted in PBS 1% of BFS. Finally, cell suspensions were fixed with 2% paraformaldehyde and subjected to flow cytometry (FACS Calibur, BD Biosciences). Data were analyzed using FlowJO.

2.11. Statistical analysis

All experiments were performed in triplicate and repeated at least twice. Values were expressed as the mean ± SEM. Student T test, or Kruskal–Wallis (ANOVA) tests were used to evaluate the statistical differences between two groups or more than two groups, respectively. A p value < 0.05 was considered statistically significant. Prism 5 software (Graph Pad, San Diego, CA) was used for the analysis.

3. Results

3.1. Intraperitoneal administration of AAT decreases both retinal thinning and loss of ganglion cells

In order to determine whether AAT has a protective effect we investigated retinal thinning and ganglion cell quantity in the retina of diabetic mice. While we observed both retinal thinning and ganglion cell loss in diabetic mice, these events were markedly improved in AAT-treated mice (Figs. 1 and 2). The central retinal thinning in AAT-treated diabetic animals showed similar values to the control mouse retinas. Differences were found in the inner retina composed by, Fiber and Ganglion Cell Layer (FCL and GCL) and Inner Plexiform Layer (IPL) ($p < 0.05$) (Fig. 1A and B). No difference was found in the peripheral retina and in each of its layers (Fig. 1C and D). Moreover, 8 weeks after diabetes induction by streptozotocin (STZ) injection we observed a significant difference in the number of central and peripheral retinal Bcrn3$^+$ nuclei in AAT-treated diabetic mice compared to diabetic animals ($p < 0.05$) (Fig. 2A and B).

3.2. Cytokines and chemokines involved in retinal remodeling induced by AAT

In order to assess if the delay of neurodegenerative changes observed in retina of AAT-treated mice was related to the inflammatory status, we analyzed several cytokines and chemokines in both serum and retinal samples using microarrays. The followings cytokines were down-regulated in serum of AAT-treated diabetic mice compared to non-treated diabetic mice: Tumor Necrosis Factor-α (TNF-α), Soluble Intercellular Adhesion Molecule-1 (sICAM-1), Interleukin-1α (IL-1α), Interleukin-1β (IL-1β), Interleukin-3 (IL-3), Interleukin-7 (IL-7), Interleukin-17 (IL-17), Interleukin-27 (IL-27), Interferon-γ (INF-γ), Macrophage Inflammatory Protein-1 alpha (MIP-1a/CCL3), Monocyte Induced by Gamma interferon (MIG/CXCL9), Interferon inducible T-cell Alpha Chemoattractant (I-TAC/CXCL11). The serum cytokines that were found to be up-regulated: Chemokine C-C motif ligand-1 (CCL-1), Macrophage Inflammatory Protein-2-alpha (MIP-2-α/CXCL2), Granulocyte-Colony Stimulating Factor (G-CSF). Finally, several cytokines were unmodified: Monocyte Chemoattractant Protein-1 (MCP-1/CCL2), Regulated on Activation Normal T Cell Expressed and Secreted (RANTES/CCL5), Chemokine (C-X-C motif) ligand-1 (CXCL-1), Interferon gamma Induced Protein-10 (IP-10/CXCL10), Stromal cell-Derived Factor-1 (SDF-1/CXCL12), B Lymphocyte Chemoattractant (BLC/CXCL13), Interleukin-1 receptor a (IL-1ra), Interleukin-4 (IL-4), Interleukin-13 (IL-13), Interleukin-16 (IL-16), Interleukin-23 (IL-23), Complement c5 precursor (C5a), Macrophage Colony Stimulator Factor (M-CSF) Tissue Inhibitor Metalloproteinase-1 (TIMP-1), Triggering receptor expressed on myeloid cells-1 (TREM-1) (Table 1 and Fig. S2). There were 10 cytokines not detected. As a result, AAT was able to induce downregulation of the most potent inflammatory cytokines TNF-α, IL-1α, IL-1β, and soluble integrin ICAM ($p < 0.05$ AAT-treated vs. untreated diabetic mice) (Fig. S2).

At the retina level we observed that IL-3 was down-regulated; and MIP-1a/CCL3 and RANTES/CCL5 were up-regulated in AAT-treated diabetic compared with non-treated diabetic mice; ($p < 0.05$; AAT-treated vs. untreated diabetic mice; Student's T test). Also, as well as serum, several cytokines showed no changes: CXCL2, MIG/CXCL9, IP-10/CXCL10, I-TAC/CXCL11, SDF-1/CXCL12, BLC/CXCL13, IL-1ra, IL-4, IL-7, IL-13, IL-17, IL-27, C5a, sICAM-1, IFN-γ, M-CSF, TIMP-1 and

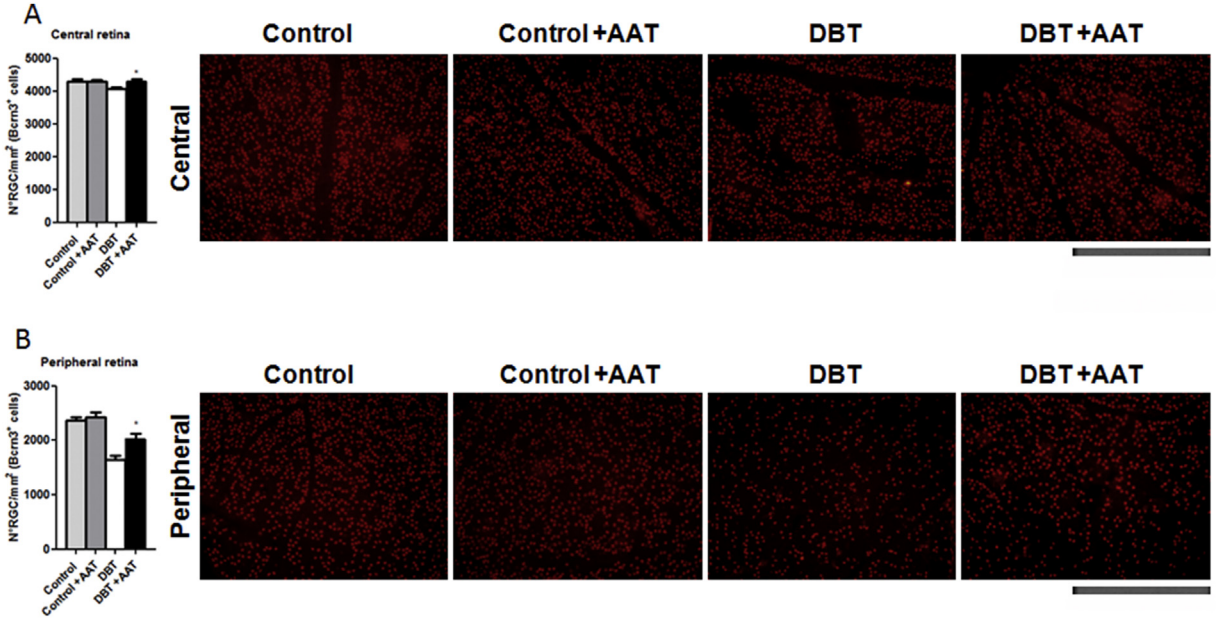

Fig. 2. Retinal ganglion cell analysis. Images are representative of Brn3a$^+$ immunostaining in flat-mounted retinas in (A) central retina and (B) peripheral retina. Ganglion cells quantification (NRGCs/mm^2) in all experimental groups. Differences were founded between DBT and DBT + AAT mice ($p < 0.05$; ANOVA, Kruskal-Wallis test). Scale bar: 50 μm.

Table 1
Serum cytokines.

Serum fold change					
Chemokines	RefSeq	+AAT	DBT	DBT + AAT	Description
Down-regulated					
TNF-α	NP_038721.1	−3.80 ± 0.02	−1.30 ± 0.77	−3.19 ± 0.07	Potent proinflamatory cytokine. Secreted by macrophages. Endothelium activation.
sICAM-1	NP_034623.1	−1.88 ± 0.01	1.00 ± 0.93	−2.03 ± 0.01	Binds LFA-1. It participates in the innate immune response
IL-1α	NP_034684.2	−4.18 ± 0.01	−1.29 ± 0.63	−8.57 ± 0.09	Produced by activated macrophages. Are involved in the inflammatory response
IL-1β	NP_032387.1	−4.76 ± 0.02	−5.33 ± 0.38	−7.19 ± 0.14	Potent proinflammatory cytokine induces neutrophil influx.
IL-3	NP_034686.2	−4.14 ± 0.01	−3.73 ± 0.26	−2.01 ± 0.39	Induces granulocytes, macrophages, mast cells, stem cells, eosinophils.
IL-7	NP_001300817.1	−5.22 ± 0.06	−4.30 ± 0.19	−11.17 ± 0.03	Hematopoietic growth factor. Stimulate the proliferation of lymphoid progenitors.
IL-17	NP_034682.1	−7.79 ± 0.04	−1.87 ± 0.45	−20.09 ± 0.03	Pro-inflammatory. Produced by activated T-cells and cells of innate immune
IL-27	NP_663611.1	−5.53 ± 0.02	−2.75 ± 0.52	−12.57 ± 0.07	Pro-/anti-inflammatory. Suppresses production of IL2, IL4, IL5 and IL6
IFN-γ	NP_032363.1	−5.14 ± 0.3	−1.52 ± 0.67	−3.79 ± 0.08	Is secreted by cells of both the innate and adaptive immune systems.
CCL3	NP_035467.1	−6.23 ± 0.1	−3.63 ± 0.21	−6.44 ± 0.14	Potent chemotactic activity for eosinophils.
CXCL9	NP_032625.2	−5.94 ± 0.01	−1.85 ± 0.48	−2.54 ± 0.19	Affects the growth, movement, or activation state of cells in inflammatory response.
CXCL11	NP_062367.1	−4.63 ± 0.1	−1.77 ± 0.64	−21.25 ± 0.03	Chemotactic for monocytes, activated T-cells, or neutrophils.
Up-regulated					
CCL1	NP_035459.1	−2.79 ± 0.01	−1.58 ± 0.47	8.03 ± 2.98	Secreted by activated T cells and have chemotactic activity for monocytes.
CXCL2	NP_033166.1	−2.45 ± 0.01	−1.79 ± 0.72	3.60 ± 1.66	Chemotactic for human polymorphonuclear leukocytes.
G-CSF	NP_034101.1	−3.08 ± 0.01	−2.61 ± 0.30	3.70 ± 2.30	Production, differentiation, and function of granulocytes and macrophages
Unmodify					
CCL2	NP_035463.1	−1.58 ± 0.01	−1.40 ± 0.54	1.54 ± 0.44	Displays chemotactic activity for monocytes and memory T cells.
CCL5	NP_038681.2	−2.09 ± 0.01	1.26 ± 1.20	−1.11 ± 0.23	Chemoattractant. Eosinophils, monocytes, memory T cells, B, NK, and DCs
CXCL1	NP_032202.1	−1.65 ± 0.01	−1.07 ± 0.97	−1.16 ± 0.07	Responsible to recruit neutrophils.
CXCL10	NP_067249.1	−2.73 ± 0.01	−1.29 ± 0.73	1.22 ± 0.27	A chemoattractant for activated T cells
CXCL12	NP_001012495.1	−1.56 ± 0.01	1.11 ± 0.84	−1.16 ± 0.09	Immune surveillance, inflammation response, tissue homeostasis, and tumor growth.
CXCL13	NP_061354.1	−2.18 ± 0.01	−2.12 ± 0.44	1.22 ± 0.01	CXCR5 CXCR3 CCR10 chemokine receptor binding
IL-1ra	NP_001116854.1	−2.28 ± 0.01	−1.04 ± 0.72	−1.08 ± 0.04	Inhibits the activity of interleukin-1 by binding to receptor IL1R1.
IL-4	NP_067258.1	−7.00 ± 0.2	−4.11 ± 0.17	−2.58 ± 0.33	B-cell activation processes as well as of other cell types
IL-13	NP_032381.1	−2.46 ± 0.1	−1.93 ± 0.40	−1.41 ± 0.36	Inhibits inflammatory cytokine production. Regulating interferon-gamma synthesis.
IL-16	NP_034681.2	−2.20 ± 0.01	−1.60 ± 0.64	1.25 ± 0.47	Stimulates a migratory response in monocytes, $CD4^+$ cells, and eosinophils
IL-23	NP_112542.1	−1.48 ± 0.09	−3.68 ± 0.27	−1.32 ± 0.75	Associates with IL12B. Promotes production of proinflammatory cytokines
c5/c5a	NP_034536.2	−2.75 ± 0.01	−2.64 ± 0.37	1.28 ± 0.01	Complement system. Anaphylatoxin, which possesses potent chemotactic activity
M-CSF	NP_001107001.1	−3.07 ± 0.01	1.05 ± 0.96	−1.46 ± 0.03	Survival, proliferation and differentiation of macrophages.
TIMP-1	NP_001037849.1	−2.00 ± 0.01	−1.27 ± 0.80	1.30 ± 0.27	Metalloproteinase inhibitor. Regulates cell differentiation, migration and cell death
TREM-1	NP_001334328.1	−3.32 ± 0.01	1.04 ± 0.77	1.79 ± 0.07	Multifunctional proinflammatory cytokine that belongs to the tumor necrosis factor

Cytokines and chemokines down-regulated: Tumor Necrosis Factor-α (TNF-α), soluble Intercellular Adhesion Molecule-1 (sICAM-1), Interleukin-1α (IL-1α), Interleukin-1β (IL-1β), Interleukin-3 (IL-3), Interleukin-7 (IL-7), Interleukin-17 (IL-17), Interleukin-27 (IL-27), Interferon-γ (INF-γ), Macrophage Inflammatory Protein-1 alpha (MIP-1a/CCL3), Monocyte Induced by Gamma interferon (MIG/CXCL9), Interferon inducible T-cell Alpha Chemoattractant (I-TAC/CXCL11), ($p < 0.05$ DBT vs. DBT + AAT; Student's T test).
Cytokines up-regulated: Chemokine (C-X-C motif) ligand-1 (CXCL-1), Granulocyte-Colony Stimulating Factor (G-CSF), Macrophage Inflammatory Protein-2-alpha (MIP-2-alpha/CXCL2) ($p < 0.05$ DBT vs. DBT + AAT; Student's T test). *Cytokines and chemoquines unmodify*: Monocyte Chemoattractant Protein-1 (MCP-1/CCL2), RANTES/CCL5 (Regulated on Activation, Normal T Cell Expressed and Secreted), KC/CXCL1 (C-X-C motif ligand-1), Interferon gamma Induced Protein-10 (IP-10/CXCL10), Stromal cell-derived factor-1 (SDF-1/CXCL12), B Lymphocyte Chemoattractant (BLC/CXCL13), Interleukin-1ra (IL-1ra), Interleukin-4 (IL-4), Interleukin-13 (IL-13), Interleukin-16 (IL-16), Interleukin-23 (IL-23), Complement component 5a (c5/c5a), Macrophage-Colony Stimulating Factor (M-CSF), Tissue Inhibitor Metalloproteinase-1 (TIMP-1), Triggering receptor expressed on myeloid cells-1 (TREM-1) (http://www.uniprot.org/2002–2018).

TREM-1. The remaining cytokines were not detected in any animal groups (Table 2 and Fig. S2).

3.3. AAT modulates the serum and retina level of TNF- α

Different studies have shown that the inflammatory cytokine TNF-α is increased in the retina (Joussen et al., 2002) and vitreous of diabetic mice. Furthermore, TNF-α was also found to be increased in patients with DR (Doganay et al., 2002; Demircan et al., 2006). Recent research (Wang et al., 2017) showed that an i.p. injection of AAT was able to decrease the serum level of TNF-α in diabetic animals. In order to confirm the reduced expression of TNF-α found by the microarray assay in serum we analyzed the level of TNF-α in AAT-treated and non-treated diabetic mice by ELISA. We observed that both retinal and serum levels of TNF-α were significantly increased in non-treated diabetic animals while diabetic AAT-treated showed reduced TNF-α levels reaching values of healthy (control) mice ($p < 0.05$ AAT-treated vs. untreated diabetic mice ANOVA; Kruskal-Wallis test) (Fig. 3A and B).

3.4. The percentage of $CD11b^+F4/80^+$ macrophages is increased in the retina of diabetic animals

It has been described that F4/80 is a good marker for murine macrophages (Martinez and Gordon, 2014; Gordon and Pluddemann, 2017). Regarding that retina upregulated cytokines are monocyte chemotactic CCL3 and CCL5 (Table 2), we decided first to evaluate the levels of *f4/80* transcripts in the whole retina. We found that mRNA levels of *f4/80* were increased in both diabetic AAT-treated and diabetic non-treated groups compared to controls ($p < 0.05$ ANOVA; Kruskall-Wallis test; Fig. 4A). Then, we determined the percentage of $CD11b^+F4/80^+$ cells in all experimental groups by flow cytometry. We found that $CD11b^+F4/80^+$ cells were increased in diabetic group and an increase trend in AAT-treated diabetic group compared to control mice. No significant differences were seen among diabetic and AAT-treated diabetic groups ($p < 0.05$ Control vs. diabetic and control vs. AAT-treated diabetic mice, ANOVA; Kruskal-Wallis test) (Fig. 4B).

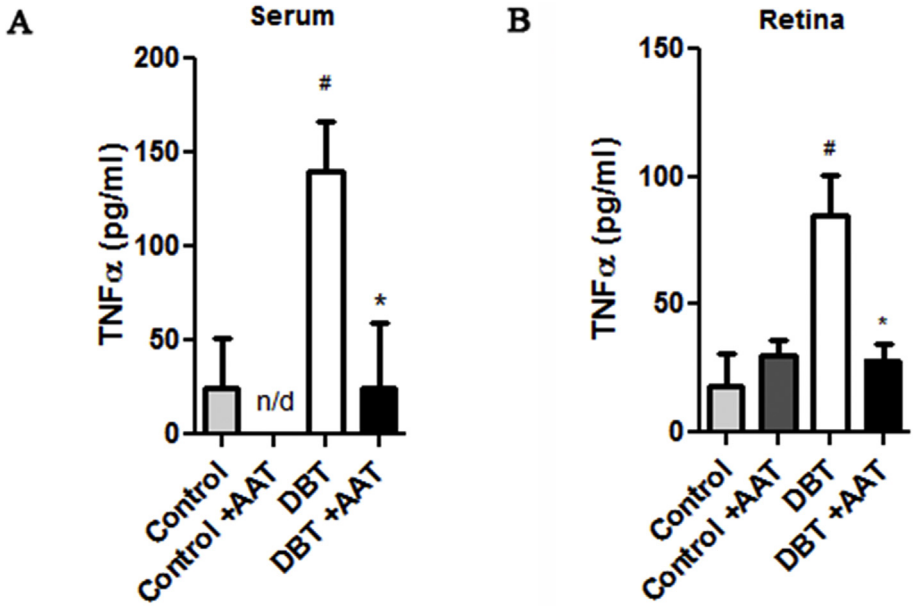

Fig. 3. TNF-α level quantified by ELISA were found higher in DBT mice compared with control (healthy mice), while were significantly reduced in DBT + AAT mice both (A) serum and (B) retina (#p < 0.05 Control vs. DBT, **p < 0.05 DBT vs. DBT + AAT; ANOVA, Kruskal-Wallis test).

Table 2
Cytokines and chemokines in the retina.

Retina fold change					
Chemokines	RefSeq	+AAT	DBT	DBT + AAT	Description
Down-regulated					
IL-3	NP_034686.2	1.12 ± 0,03	12.30 ± 0,23	−13.21 ± 0,01	Induces granulocytes, macrophages, mast cells, stem cells, erythroid cells, eosinophils.
Up-regulated					
CCL3	NP_035467.1	1.00 ± 0,04	5.41 ± 0,23	3.20 ± 0,03	Potent chemotactic activity for eosinophils.
CCL5	NP_038681.2	1.00 ± 0,04	2.38 ± 0,09	3.14 ± 0,07	Chemoattractant eosinophils, basophils, monocytes, memory T cells, B, NK and DCs
Unmodify					
CXCL2	NP_033166.1	−1.49 ± 0,41	1.13 ± 0,34	1.67 ± 1,12	Chemotactic for human polymorphonuclear leukocytes.
CXCL9	NP_032625.2	1.32 ± 0,50	3.94 ± 0,43	1.12 ± 0,08	Affects the growth, movement, or activation state of cells in inflammatory response.
CXCL10	NP_067249.1	1.01 ± 0,78	15.90 ± 0.34	−8.84 ± 6.90	A chemoattractant for activated T cells.
CXCL11	NP_062367.1	1.04 ± 0,43	5.10 ± 0,56	−1.18 ± 1,10	Chemotactic for monocytes, activated T-cells, or neutrophils.
CXCL12	NP_001012495.1	1.71 ± 0,53	2.41 ± 0,12	−2.45 ± 1.54	Immune surveillance, inflammation response, tissue homeostasis, and tumor growth.
CXCL13	NP_061354.1	18.01 ± 0,70	11.21 ± 0,19	1.36 ± 1,23	CXCR5 CXCR3 CCR10 chemokine receptor binding
IL-1ra	NP_001116854.1	2.74 ± 0,90	1.25 ± 0,98	1.55 ± 1,20	Inhibits the activity of interleukin-1 by binding to receptor IL1R1.
IL-4	NP_067258.1	1.00 ± 0,65	18.70 ± 2,89	−1.41 ± 0,93	Participates in at least several B-cell activation processes as well as of other cell types
IL-7	NP_001300817.1	1.74 ± 0,95	2.70 ± 1,10	−1.27 ± 0,87	Hematopoietic growth factor capable of stimulating the proliferation of lymphoid progenitors.
IL-13	NP_032381.1	1.19 ± 0,01	4.17 ± 2,10	1.61 ± 0,79	Inhibits inflammatory cytokine production. Regulating interferon-gamma synthesis.
IL-17	NP_034682.1	3.76 ± 0,03	5.86 ± 0,12	−1.91 ± 090	Pro-inflammatory. Produced by activated T-cells and cells of innate immune
IL-27	NP_663611.1	1.41 ± 0,09	3.09 ± 0,16	−2.25 ± 1.23	Pro-/anti-inflammatory.Suppresses production of IL2, IL4, IL5 and IL6
c5/c5a	NP_034536.2	7.85 ± 2,21	10.22 ± 0,19	−1.44 ± 0,89	Complement system. Anaphylatoxin which possesses potent chemotactic activity
sICAM-1	NP_034623.1	1.31 ± 1,12	1.60 ± 0,29	1.26 ± 0,76	Binds leukocyte adhesion protein LFA-1. It participates in the innate immune response
IFN-γ	NP_032363.1	2.16 ± 0,09	2.00 ± 1,10	1.35 ± 0,91	Is secreted by cells of both the innate and adaptive immune systems.
M-CSF	NP_001107001.1	2.85 ± 0,45	5.74 ± 2,18	−1.51 ± 0,16	Survival, proliferation and differentiation of macrophages.
TIMP-1	NP_001037849.1	−2.84 ± 0,64	2.83 ± 1,14	−1.52 ± 0,98	Metalloproteinase inhibitor. Regulates cell differentiation, migration and cell death
TREM-1	NP_001334328.1	1.03 ± 0,01	1.12 ± 0,16	3.11 ± 1,68	Multifunctional proinflammatory cytokine that belongs to the tumor necrosis factor

Cytokines and chemokines down-regulated: Interleukin-3 (IL-3).
Cytokines up-regulated: Macrophage Inflamatory Protein-1 alpha (MIP-1a/CCL3), Regulated on Activation, Normal T Cell Expressed and Secreted (RANTES/CCL5).
Citokynes and chemoquines unmodify: Macrophage Inflammatory Protein-2-alpha (MIP-2-alpha/CXCL2), Monocyte Induced by Gamma interferon (MIG/CXCL9), Interferon gamma Induced Protein-10 (IP-10/CXCL10), Interferon inducible T-cell Alpha Chemoattractant (I-TAC/CXCL11), stromal cell-derived factor-1 (SDF-1/CXCL12), B Lymphocyte Chemoattractant (BLC/CXCL13), Interleukin-1ra (IL-1ra), Interleukin-4 (IL-4), Interleukin-7 (IL-7), Interleukin-13 (IL-13), Interleukin-17 (IL-17), Interleukin-27 (IL-27), Complement component 5a (c5/c5a), soluble Intercellular Adhesion Molecule-1 (sICAM-1), Interferon-γ (INF-γ), Macrophage-Colony Stimulating Factor (M-CSF), Tissue Inhibitor Metalloproteinase-1 (TIMP-1), Triggering receptor expressed on myeloid cells-1 (TREM-1) (http://www.uniprot.org/ 2002–2018).

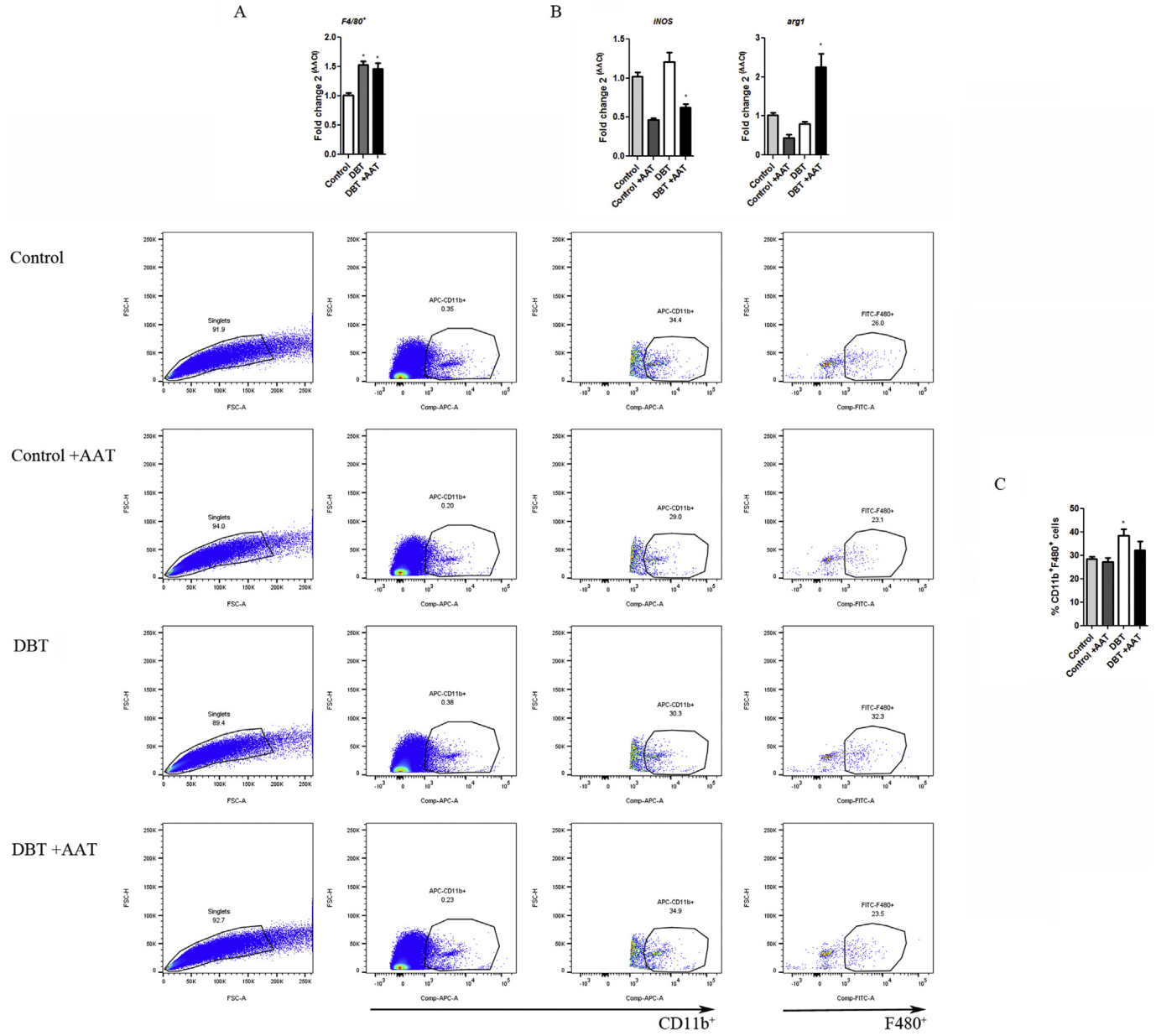

Fig. 4. AAT and macrophages in the retina. (A) Fold changes of *f4/80* mRNA ($p < 0.05$; Control vs. DBT and DBT + AAT; ANOVA; Kruskall-Wallis test). (B) $CD11b^{+}F4/80^{+}$ cells from whole retina. Representative Zebraplots from $CD11b^{+}F4/80^{+}$ cells in different groups were obtained from gated single-cell population, the second gating was performed in a two-step fashion in $CD11b^{high}$ cells (gating between dash), finally the $CD11b^{high}$ positive population was gated in $F480^{+}$ cells ($p < 0.05$ Control vs. DBT and control vs. DBT + AAT mice, ANOVA; Kruskal-Wallis test). (C) Analysis of mRNA levels of inducible nitric oxidase syntase (*iNOS*) and *arginase 1* (*arg1*) of the whole retina (*iNOS*: $p < 0.05$; Control vs. Control + AAT, and $p < 0.05$ DBT vs. DBT + AAT; *arg1*: DBT vs. DBT + AAT: ANOVA; Kruskal-Wallis test).

3.5. Macrophage-microenvironment profile of AAT-treated mice

In order to characterize the retinal microenvironment where the $F4/80^{+}$ cells were found, a real-time PCR of the whole retina for *iNOS* and *arg1* genes was performed in the different treatments groups. The expression of *iNOS* mRNA was found to be 0.46 fold lower in diabetic AAT-treated group compared to diabetic untreated mice ($p < 0.05$; AAT-treated vs. untreated diabetic mice; ANOVA; KruskalWallis test). Unexpectedly we found similar differences between control and control AAT-treated mice, suggesting that AAT has an effect independent of diabetes condition ($p < 0.05$; AAT-treated vs. untreated control mice; ANOVA; Kruskal-Wallis test). Importantly, *arg1* was found to be 2.65 fold higher in AAT-treated animals (Fig. 4C) ($p < 0.05$; AAT-treated vs. untreated diabetic mice; ANOVA; Kruskal-Wallis test), indicating an anti-inflammatory profile in the retinal milieu.

3.6. AAT modulates macrophage phenotype toward M2 in vivo and in vitro

M2 macrophages are characterized by a lower expression of *iNOS* and an elevated expression of a*rg1,* and expressed the mannose receptor CD206 as well (Gordon and Pluddemann, 2017). We therefore carried out flow cytometry analysis for $F4/80^{+}$ and $CD206^{+}$ on retina samples of mice from all experimental groups. We observed that macrophages $CD206^{+}F4/80^{+}$ double positive cells were increased in the retina of AAT-treated diabetic mice (Fig. 5) ($p < 0.05$; AAT-treated vs. untreated diabetic mice; ANOVA; Kruskal-Wallis test). Collectively, these results suggest that AAT was capable to modulate the macrophage profile toward a M2 phenotype without modifying the percentage of

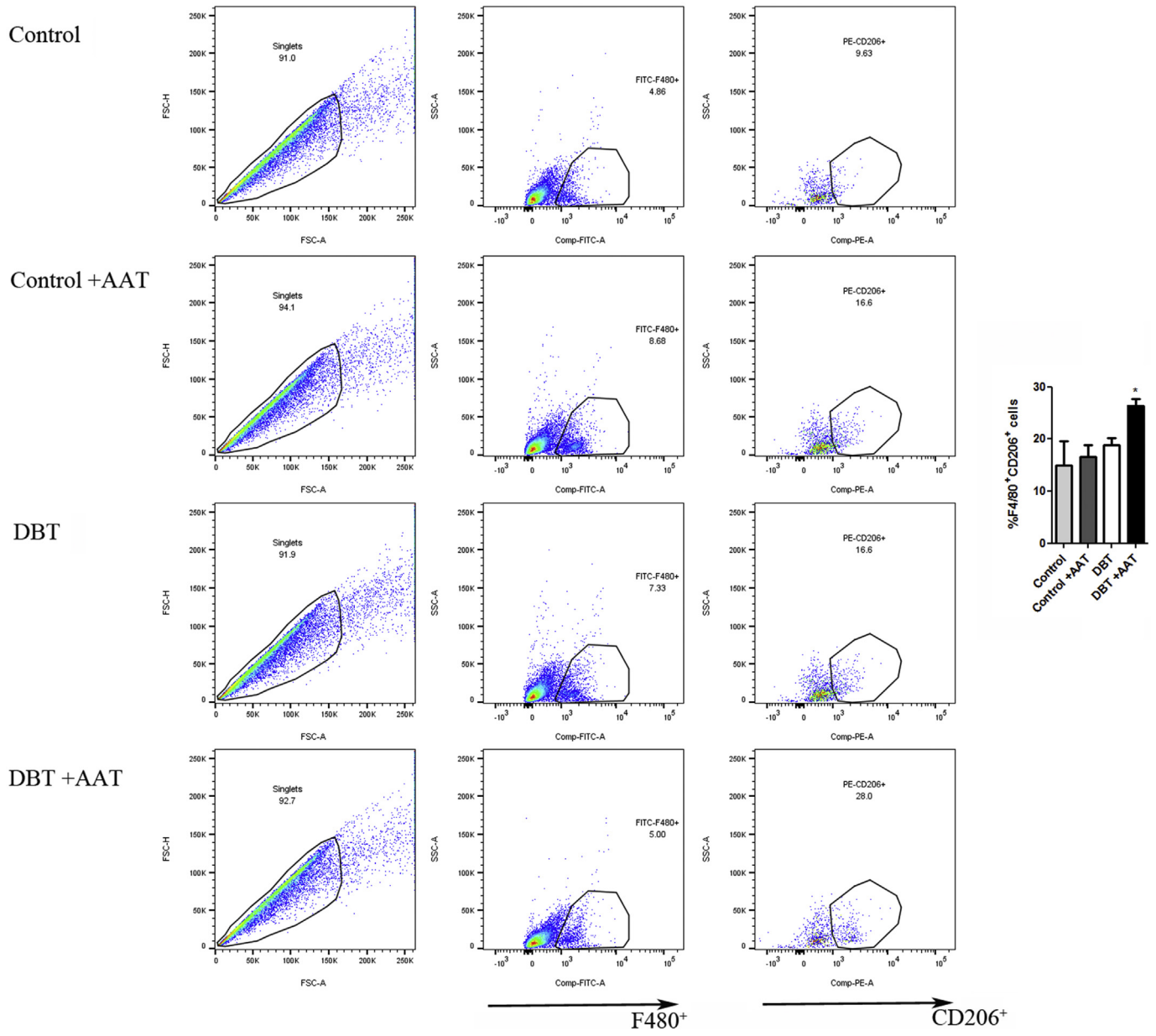

Fig. 5. Phenotype of retinal macrophages. (A) Representative dot plots of double positive F4/80$^+$CD206$^+$ cells of the whole retina were obtained using gated regions: single-cell population and F4/80$^+$ cells; (upper panel). CD206$^+$ cells were increased in DBT and more significantly in DBT + AAT ($p < 0.05$; DBT vs. DBT + AAT; ANOVA; Kruskal-Wallis test).

F4/80$^+$ cells in the retina of treated mice.

Investigations reported that AAT can modulate the inflammatory profile of different types of cells (Ozeri et al., 2012; Gottlieb et al., 2014). Therefore, we decided to evaluate whether AAT was able to modulate the profile *in vitro* of macrophage cell lines Raw264.1 and J774.2. Surprisingly, we found that AAT could modulate CD206 expression in both cell lines. A slightly increase of CD206 expression of Raw264.1 and J774.2 cells exposed to AAT was observed (Fig. 6C and D) ($p < 0.05$, Control vs. 4.5 mg/ml AAT, Student's T test).

3.7. Toxicology parameters during AAT treatment

Finally, we assessed the toxicology profile of AAT administration in mice and found that the scheme applied was well tolerated with no evident signs of clinical, biochemical or hematological toxicity within the studied period of time (Fig. 7). We did not find differences in systemic leukocyte number between groups (Fig. 7A) or in levels of aspartate transaminase (AST) and alanine aminotransferase (ALT) hepatic enzymes (Fig. 7B and C) ($p < 0.05$, ANOVA, Kruskall-Wallis).

4. Discussion

We have carried out a research study on the use of AAT to prevent neurodegenerative and inflammatory changes in the retina of type 1 diabetes mice. At 8 weeks of diabetes AAT treated animals had less ganglion cells loss, a thicker retina, a group of downregulated pro-inflammatory cytokines, decreased levels of TNF-α in serum and retina as well as an anti-inflammatory profile of the retinal microenvironment of macrophage cells. It has been widely reported that a chronic and progressing neurodegenerative process starts early in the diabetic retina, both in humans and in mice (van Dijk et al., 2010; Yang et al., 2012, Tavares Ferreira et al. 2016; Srinivasan et al., 2017).

Longitudinal studies carried out in type 1 diabetic patients confirmed the presence of retinal neurodegeneration before the vascular

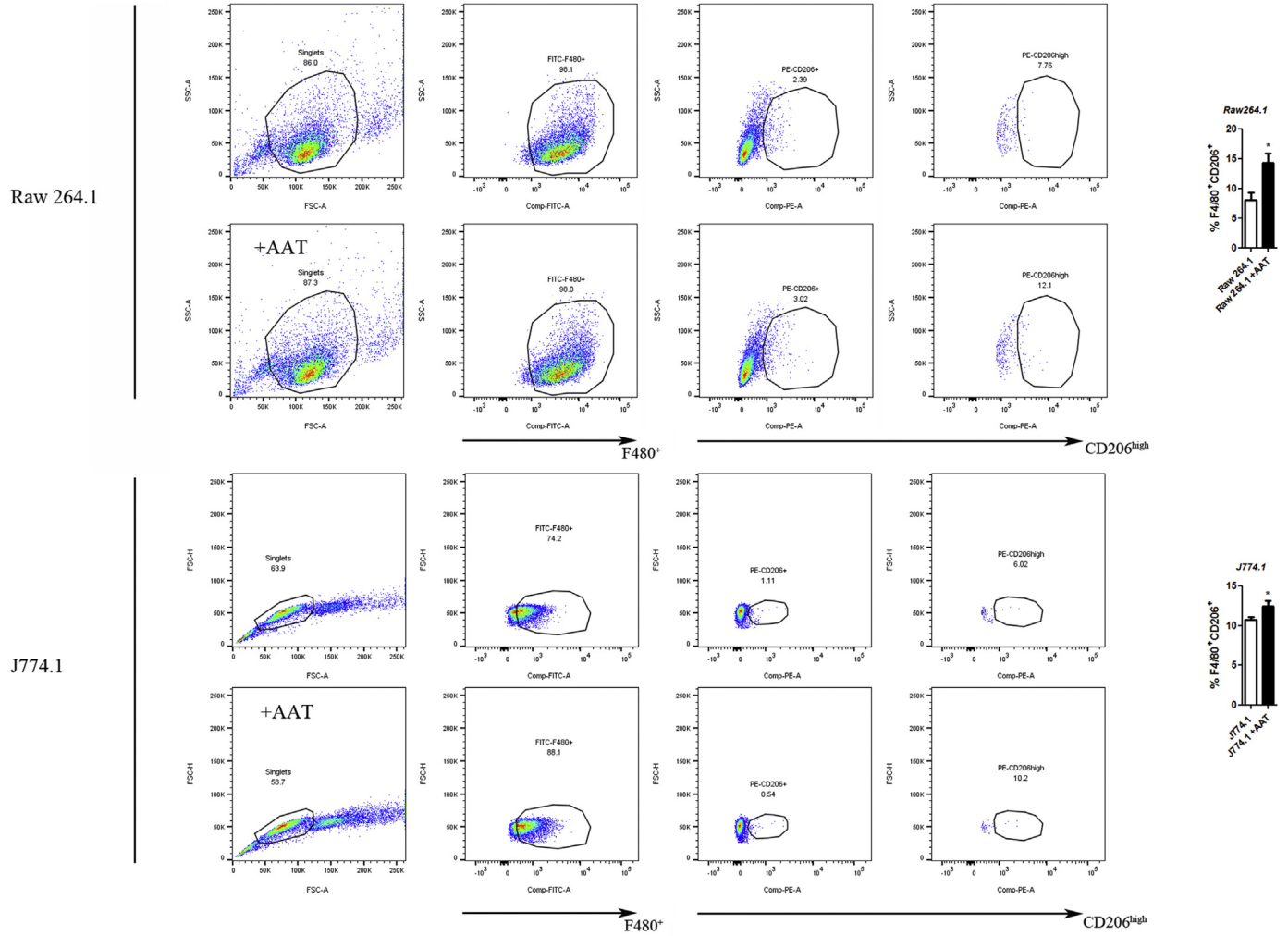

Fig. 6. Flow cytometry of (A) Raw 264.1 and (B) J774.2 macrophages cells treated or not with 4.5 mg/ml AAT ON. Representative Zebraplots of control and AAT-treated cells (+AAT) for both cell lines. Raw: *p < 0.05 Control vs. AAT-treated cells; Student's T test. J774.2: *p < 0.05 Control vs. AAT-treated cells; Student's T test.

unit is affected. Particularly the inner retina was affected (van Dijk et al., 2009). Retinal thinning and ganglion cell loss occur even when the vascular component of DR remains minimally damaged in these patients (van Dijk et al., 2010; Sohn et al., 2016). It is known that Brn3+ retinal ganglion cells (RGCs) in STZ-induced diabetic mice are reduced from 6 weeks onwards and precedes microvascular changes (Martin et al., 2004; Yang et al., 2012). Also, Nuclear Fiber Layer and Ganglion Cell Layer (NFL + GCL) have been found to be thinner 6 weeks after diabetes induction (Sohn et al., 2016). In our model, we found that AAT minimized the loss of Brn3+ RGCs at 8 weeks of

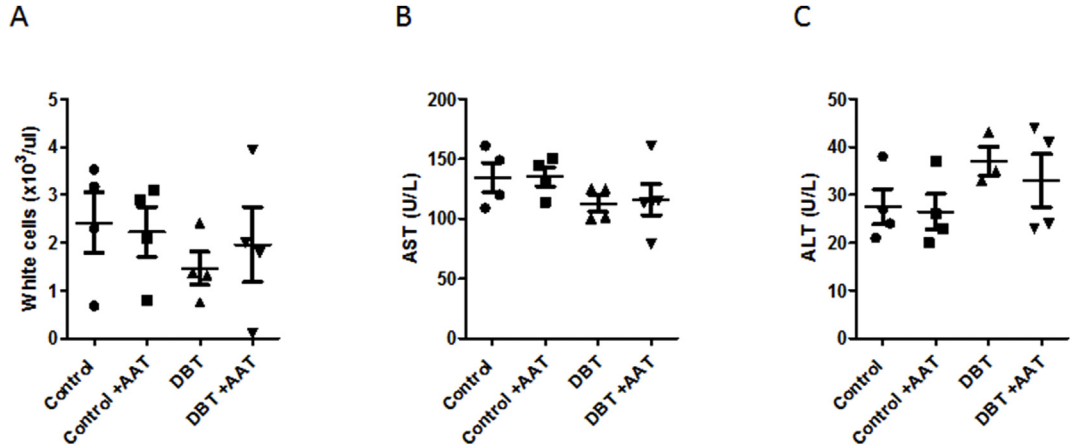

Fig. 7. (A) Determination of peripheral white cells. No differences were found between groups. (B) Analysis of hepatic enzyme AST: aspartate transaminase units (U) per liter (L) and (C) ALT: alanine aminotransferase (U/L). No differences were found between four groups analyzed.

diabetes and also delayed the thinning of inner retina (NFL, GCL and IPL). Then, we demonstrated for the first time that AAT was able to moderate retinal neurodegeneration caused by diabetes in mice.

Over the last years it has been described the role of the innate immune cells and cytokines during the complications of diabetes (Tang and Kern, 2011). In these sense, in the early stages, metabolic imbalance may be detected by macrophages that could modify its profile and secrete pro-inflammatory molecules such as IL-1β and TNF-α (Tang and Kern, 2011; Xu and Chen, 2017) leading to the activation of retinal endothelium and increase of integrins (sICAM-1) and selectins. Subsequently, activated endothelium contributes to generate leukostasis and in turn, cause non-perfusion areas. In the current study we set out to see if the early inflammatory changes caused by diabetes could be reduced by AAT. By using microarrays of cytokines and chemokines analyzed in both retina and serum, we demonstrated that lower levels of pro-inflammatory cytokines and factors TNF-α, IL1α, IL1β, INF-γ, IL-3, IL-7, IL17, IL-23, IL-27, sICAM and chemokines CXCL1, CXCL9, CXCL11, CXCL12, CCL3, CCL5, when mice received AAT. In addition, it has been reported that TNF-α, one of the main inflammatory cytokines, is increased in the serum of diabetic patients and relates to the severity of DR (Doganay et al., 2002). TNF-α has been the target of several strategies (Behl et al. 2008, 2009), especially the blockade of TNF-α that reduced leukocyte adhesion, suppressed blood retinal barrier breakdown and reduced ICAM-1 expression (Joussen et al., 2002). In this study, we demonstrated that the use of AAT reduce the levels of TNF-α both in the serum and in the retina of diabetic animals. Besides, we observed lower expression of sICAM in the serum of diabetic AAT-treated mice. Then, these findings suggest that AAT has the capability to prevent the inflammatory state.

Macrophages with a M2 profile have been described to be anti-inflammatory, with beneficial potential in different tissues (Wynn et al., 2013; Martinez and Gordon, 2014; Gordon and Pluddemann, 2017). Interestingly, a recent report showed that AAT-treated macrophages exhibit similarity to an M2-like profile (Churg et al., 2007). Here, we showed that both transcript levels of *f4/80* and $F4/80^+$ cells are higher throughout the retina of diabetic animals. This indicates an increased number of macrophages in the diabetic retina, which has been previously reported (Rangasamy et al., 2014). Surprisingly, when we focused on the inflammatory profile of these cells, we found that the retina of AAT-treated animals presented increased levels of double positive $F4/80^+CD206^+$ cells. It is well-known that M2 profile has $CD206^{high}$ surface expression (Wynn et al., 2013; Gordon and Pluddemann, 2017). Also, lower *iNOS* and higher *arg1* activity and expression have been described as a characteristic of M2 (Wynn et al., 2013). Accordingly, we showed that transcript levels of the enzymes *iNOS* were decreased while transcripts levels of *arg1* were increased in the whole retina of diabetic AAT-treated animals. It has been previously mentioned, that IL-13 and IL-4 cytokines could modulate macrophages to an M2 profile with high expression of Arginase1 in mice (Van Dyken and Locksley 2013). Interestingly, an injection of recombinant IL-13 could reduce inflammation in LPS-induced eye humor aqueous of rats (Lemaitre et al., 2001). In our study we found higher levels of IL-13 in the retina of AAT-treated animals suggesting a possible mechanism. Another M2 cytokine is IL-10 which was not detected; perhaps it means that those animals have a lower inflammatory state. Collectively our *in vivo* findings about $CD206^{high}$ cells, *iNOS*, *arg1*, the retinal expression of IL-13 and lower levels of retinal TNF-α, strongly support the idea that AAT could modulate macrophages phenotype to an M2 profile. In addition, we observed that *in vitro* AAT-treated Raw 264.1 and J774.2 macrophages increased the percentage of $CD206^+$ cells in comparison with untreated cells. Then, AAT had the ability to modulate the macrophage to an anti-inflammatory profile both *in vivo* and *in vitro* and to decrease the production of pro-inflammatory cytokines as we observed in the *in vivo* model. These mechanisms triggered by AAT might have influenced and prevented retinal thinning and ganglion cell loss.

In this model, we have also seen that AAT-treated animals showed upregulation of retinal CCL3, CCL5 as well as systemic CCL1. These cytokines are chemo-attractant for several types of cells including macrophages (Luster, 1998; Olson and Ley, 2002) and may be responsible for the increase trend in the number of $CD11b^+F4/80^+$ cells in the retina of AAT-treated diabetic mice as we showed in this work. Importantly, no differences were seen in all white blood cells. Nevertheless, we hypothesize that an increased number of macrophages in the retina may not be detrimental of the disease if they are predominantly M2, considering their capability to disrupt the pro-inflammatory context observed in early diabetes and to maintain an anti-inflammatory microenvironment which in turn reflects in better clinical outcomes. Additionally, we suggest that the administration of AAT might be beneficial not only in our animal model, also in other models that need to boost the regenerative or anti-inflammatory capacity of macrophages with a M2 profile or even for patients with DR. In fact, a clinical trial of AAT and diabetes performed in young patients showed that AAT-treated patients had a trend toward better metabolic control than that observed in non-AAT treated diabetics (Phase 2 trial of Alpha-1 Antitrypsin (AAT) in newly diagnosed type-1 diabetes (T1D) patients; Clinical Trial NCT02005848).

5. Conclusion

In our study we have observed beneficial effects of AAT in the retina and also systemically in type 1 diabetic animals. We think AAT is an interesting molecule to be tested in diabetic retinopathy. However, further investigation is necessary to evaluate this potentially beneficial effect.

Author contributions statement

Gustavo Ortiz (GO).
Emiliano López (EL).
Juan Pablo Salica (JPS).
Constanza Potilinski (CP).
Mariano Fernández Acquier (MFA).
Eduardo Chuluyan (EC).
Juan Eduardo Gallo (JEG).

GO conceived all the experiments. GO, EL, JPS, CP, MFA, EC, JEG analyzed the results and all authors reviewed the manuscript.

Competing financial interest statement

All authors deny having any competing financial interests regarding the present manuscript.

Financial support

Research Grants from Universidad Austral and Agencia Nacional de Promocion Cientifica y Tecnologica (PICTO, 2016–0105).

Conflicts of interest

The authors of this work declare that they do not have any conflicts of interest.

Acknowledgments

We want to special thank to Angie Garriz. Also want to thank Guillermo Gastón, Mariana Banis and Norma Montalbetti.

Appendix A. Supplementary data

Supplementary data related to this article can be found at http://dx.doi.org/10.1016/j.exer.2018.05.013.

References

Abcouwer, S.F., Antonetti, D.A., 2013. A role for systemic inflammation in diabetic retinopathy. Invest. Ophthalmol. Vis. Sci. 54 (3), 2384.

Antonetti, D.A., Klein, R., Gardner, T.W., 2012. Diabetic retinopathy. N. Engl. J. Med. 366 (13), 1227–1239.

Behl, Y., Krothapalli, P., Desta, T., DiPiazza, A., Roy, S., Graves, D.T., 2008. Diabetes-enhanced tumor necrosis factor-alpha production promotes apoptosis and the loss of retinal microvascular cells in type 1 and type 2 models of diabetic retinopathy. Am. J. Pathol. 172 (5), 1411–1418.

Behl, Y., Krothapalli, P., Desta, T., Roy, S., Graves, D.T., 2009. FOXO1 plays an important role in enhanced microvascular cell apoptosis and microvascular cell loss in type 1 and type 2 diabetic rats. Diabetes 58 (4), 917–925.

Bystrom, J., Evans, I., Newson, J., Stables, M., Toor, I., van Rooijen, N., Crawford, M., Colville-Nash, P., Farrow, S., Gilroy, D.W., 2008. Resolution-phase macrophages possess a unique inflammatory phenotype that is controlled by cAMP. Blood 112 (10), 4117–4127.

Chakravarthy, H., Beli, E., Navitskaya, S., O'Reilly, S., Wang, Q., Kady, N., Huang, C., Grant, M.B., Busik, J.V., 2016. Imbalances in mobilization and activation of pro-inflammatory and vascular reparative bone marrow-derived cells in diabetic retinopathy. PLoS One 11 (1) e0146829.

Churg, A., Wang, X., Wang, R.D., Meixner, S.C., Pryzdial, E.L., Wright, J.L., 2007. Alpha1-antitrypsin suppresses TNF-alpha and MMP-12 production by cigarette smoke-stimulated macrophages. Am. J. Respir. Cell Mol. Biol. 37 (2), 144–151.

Cosio, M.G., Saetta, M., Agusti, A., 2009. Immunologic aspects of chronic obstructive pulmonary disease. N. Engl. J. Med. 360 (23), 2445–2454.

Demircan, N., Safran, B.G., Soylu, M., Ozcan, A.A., Sizmaz, S., 2006. Determination of vitreous interleukin-1 (IL-1) and tumour necrosis factor (TNF) levels in proliferative diabetic retinopathy. Eye (Lond) 20 (12), 1366–1369.

Doganay, S., Evereklioglu, C., Er, H., Turkoz, Y., Sevinc, A., Mehmet, N., Savli, H., 2002. Comparison of serum NO, TNF-alpha, IL-1beta, sIL-2R, IL-6 and IL-8 levels with grades of retinopathy in patients with diabetes mellitus. Eye (Lond) 16 (2), 163–170.

Van Dyken, S.J., Locksley, R.M., 2013. Interleukin-4- and interleukin-13-mediated alternatively activated macrophages: roles in homeostasis and disease. Annu. Rev. Immunol. 31, 317–343.

Edgar, R.G., Patel, M., Bayliss, S., Crossley, D., Sapey, E., Turner, A.M., 2017. Treatment of lung disease in alpha-1 antitrypsin deficiency: a systematic review. Int. J. Chronic Obstr. Pulm. Dis. 12, 1295–1308.

Gonzalez Fleitas, M.F., Bordone, M., Rosenstein, R.E., Dorfman, D., 2015. Effect of retinal ischemia on the non-image forming visual system. Chronobiol. Int. 32 (2), 152–163.

Gordon, S., Pluddemann, A., 2017. Tissue macrophages: heterogeneity and functions. BMC Biol. 15 (1), 53.

Gottlieb, P.A., Alkanani, A.K., Michels, A.W., Lewis, E.C., Shapiro, L., Dinarello, C.A., Zipris, D., 2014. alpha1-Antitrypsin therapy downregulates toll-like receptor-induced IL-1beta responses in monocytes and myeloid dendritic cells and may improve islet function in recently diagnosed patients with type 1 diabetes. J. Clin. Endocrinol. Metab. 99 (8), E1418–E1426.

Guttman, O., Baranovski, B.M., Schuster, R., Kaner, Z., Freixo-Lima, G.S., Bahar, N., Kalay, N., Mizrahi, M.I., Brami, I., Ochayon, D.E., Lewis, E.C., 2015. Acute-phase protein alpha1-anti-trypsin: diverting injurious innate and adaptive immune responses from non-authentic threats. Clin. Exp. Immunol. 179 (2), 161–172.

Hazra, S., Jarajapu, Y.P., Stepps, V., Caballero, S., Thinschmidt, J.S., Sautina, L., Bengtsson, N., Licalzi, S., Dominguez, J., Kern, T.S., Segal, M.S., Ash, J.D., Saban, D.R., Bartelmez, S.H., Grant, M.B., 2013. Long-term type 1 diabetes influences haematopoietic stem cells by reducing vascular repair potential and increasing inflammatory monocyte generation in a murine model. Diabetologia 56 (3), 644–653.

http://www.uniprot.org/. (2002-2018). "The mission of UniProt is to provide the scientific community with a comprehensive, high-quality and freely accessible resource of protein sequence and functional information.".

Hurley, K., Reeves, E.P., Carroll, T.P., McElvaney, N.G., 2016. Tumor necrosis factor-alpha driven inflammation in alpha-1 antitrypsin deficiency: a new model of pathogenesis and treatment. Expet Rev. Respir. Med. 10 (2), 207–222.

Jonigk, D., Al-Omari, M., Maegel, L., Muller, M., Izykowski, N., Hong, J., Hong, K., Kim, S.H., Dorsch, M., Mahadeva, R., Laenger, F., Kreipe, H., Braun, A., Shahaf, G., Lewis, E.C., Welte, T., Dinarello, C.A., Janciauskiene, S., 2013. Anti-inflammatory and immunomodulatory properties of alpha1-antitrypsin without inhibition of elastase. Proc. Natl. Acad. Sci. U. S. A. 110 (37), 15007–15012.

Joussen, A.M., Poulaki, V., Mitsiades, N., Kirchhof, B., Koizumi, K., Dohmen, S., Adamis, A.P., 2002. Nonsteroidal anti-inflammatory drugs prevent early diabetic retinopathy via TNF-alpha suppression. Faseb. J. 16 (3), 438–440.

Kocak, N., Alacacioglu, I., Kaynak, S., Ozcan, M.A., Celik, O., Yuksel, F., Piskin, O., Oner, H., Saatci, A.O., Ergin, M., 2010. Comparison of vitreous and plasma levels of vascular endothelial growth factor, interleukin-6 and hepatocyte growth factor in diabetic and non-diabetic retinal detachment cases. Ann. Ophthalmol. 42 (10–14).

Lai, A.K., Lo, A.C., 2013. Animal models of diabetic retinopathy: summary and comparison. J Diabetes Res 2013, 106594.

Laskin, D.L., Sunil, V.R., Gardner, C.R., Laskin, J.D., 2011. Macrophages and tissue injury: agents of defense or destruction? Annu. Rev. Pharmacol. Toxicol. 51, 267–288.

Lee, R., Wong, T.Y., Sabanayagam, C., 2015. Epidemiology of diabetic retinopathy, diabetic macular edema and related vision loss. Eye Vis (Lond) 2, 17.

Lemaitre, C., Thillaye-Goldenberg, B., Naud, M.C., de Kozak, Y., 2001. The effects of intraocular injection of interleukin-13 on endotoxin-induced uveitis in rats. Invest. Ophthalmol. Vis. Sci. 42 (9), 2022–2030.

Lewis, E.C., 2012. Expanding the clinical indications for alpha(1)-antitrypsin therapy. Mol. Med. 18, 957–970.

Li, Q., Verma, A., Han, P.Y., Nakagawa, T., Johnson, R.J., Grant, M.B., Campbell-Thompson, M., Jarajapu, Y.P., Lei, B., Hauswirth, W.W., 2010. Diabetic eNOS-knockout mice develop accelerated retinopathy. Invest. Ophthalmol. Vis. Sci. 51 (10), 5240–5246.

Luster, A.D., 1998. Chemokines–chemotactic cytokines that mediate inflammation. N. Engl. J. Med. 338 (7), 436–445.

Martin, P.M., Roon, P., Van Ells, T.K., Ganapathy, V., Smith, S.B., 2004. Death of retinal neurons in streptozotocin-induced diabetic mice. Invest. Ophthalmol. Vis. Sci. 45 (9), 3330–3336.

Martinez, F.O., Gordon, S., 2014. The M1 and M2 paradigm of macrophage activation: time for reassessment. F1000Prime Rep 6, 13.

Olson, T.S., Ley, K., 2002. Chemokines and chemokine receptors in leukocyte trafficking. Am. J. Physiol. Regul. Integr. Comp. Physiol. 283 (1), R7–R28.

Ortega-Gomez, A., Perretti, M., Soehnlein, O., 2013. Resolution of inflammation: an integrated view. EMBO Mol. Med. 5 (5), 661–674.

Ortiz, G., 2013. Retinal Expression of α-1-Antitrypsin (A1AT) in Diabetic and Non-diabetic Rats. ARVO. Seattle, IOVS 54.

Ozeri, E., Mizrahi, M., Shahaf, G., Lewis, E.C., 2012. alpha-1 antitrypsin promotes semimature, IL-10-producing and readily migrating tolerogenic dendritic cells. J. Immunol. 189 (1), 146–153.

Porcheray, F., Viaud, S., Rimaniol, A.C., Leone, C., Samah, B., Dereuddre-Bosquet, N., Dormont, D., Gras, G., 2005. Macrophage activation switching: an asset for the resolution of inflammation. Clin. Exp. Immunol. 142 (3), 481–489.

Rangasamy, S., McGuire, P.G., Franco Nitta, C., Monickaraj, F., Oruganti, S.R., Das, A., 2014. Chemokine mediated monocyte trafficking into the retina: role of inflammation in alteration of the blood-retinal barrier in diabetic retinopathy. PLoS One 9 (10), e108508.

Sohn, E.H., van Dijk, H.W., Jiao, C., Kok, P.H., Jeong, W., Demirkaya, N., Garmager, A., Wit, F., Kucukevcilioglu, M., van Velthoven, M.E., DeVries, J.H., Mullins, R.F., Kuehn, M.H., Schlingemann, R.O., Sonka, M., Verbraak, F.D., Abramoff, M.D., 2016. Retinal neurodegeneration may precede microvascular changes characteristic of diabetic retinopathy in diabetes mellitus. Proc. Natl. Acad. Sci. U. S. A. 113 (19), E2655–E2664.

Srinivasan, S., Dehghani, C., Pritchard, N., Edwards, K., Russell, A.W., Malik, R.A., Efron, N., 2017. Corneal and retinal neuronal degeneration in early stages of diabetic retinopathy. Invest. Ophthalmol. Vis. Sci. 58 (14), 6365–6373.

Tang, J., Kern, T.S., 2011. Inflammation in diabetic retinopathy. Prog. Retin. Eye Res. 30 (5), 343–358.

Tavares Ferreira, J., Alves, M., Dias-Santos, A., Costa, L., Santos, B.O., Cunha, J.P., Papoila, A.L., Abegao Pinto, L., 2016. Retinal neurodegeneration in diabetic patients without diabetic retinopathy. Invest. Ophthalmol. Vis. Sci. 57 (14), 6455–6460.

van Dijk, H.W., Kok, P.H., Garvin, M., Sonka, M., Devries, J.H., Michels, R.P., van Velthoven, M.E., Schlingemann, R.O., Verbraak, F.D., Abramoff, M.D., 2009. Selective loss of inner retinal layer thickness in type 1 diabetic patients with minimal diabetic retinopathy. Invest. Ophthalmol. Vis. Sci. 50 (7), 3404–3409.

van Dijk, H.W., Verbraak, F.D., Kok, P.H., Garvin, M.K., Sonka, M., Lee, K., Devries, J.H., Michels, R.P., van Velthoven, M.E., Schlingemann, R.O., Abramoff, M.D., 2010. Decreased retinal ganglion cell layer thickness in patients with type 1 diabetes. Invest. Ophthalmol. Vis. Sci. 51 (7), 3660–3665.

Viswanath, K., McGavin, D.D., 2003. Diabetic retinopathy: clinical findings and management. Community Eye Health 16 (46), 21–24.

Wang, J., Sun, Z., Gou, W., Adams, D.B., Cui, W., Morgan, K.A., Strange, C., Wang, H., 2017. alpha-1 antitrypsin enhances islet engraftment by suppression of instant blood-mediated inflammatory reaction. Diabetes 66 (4), 970–980.

Wynn, T.A., Chawla, A., Pollard, J.W., 2013. Macrophage biology in development, homeostasis and disease. Nature 496 (7446), 445–455.

Xu, H., Chen, M., 2017. Diabetic retinopathy and dysregulated innate immunity. Vis. Res. 139, 39–46.

Yang, Y., Mao, D., Chen, X., Zhao, L., Tian, Q., Liu, C., Zhou, B.L., 2012. Decrease in retinal neuronal cells in streptozotocin-induced diabetic mice. Mol. Vis. 18, 1411–1420.

Zeng, H.Y., Green, W.R., Tso, M.O., 2008. Microglial activation in human diabetic retinopathy. Arch. Ophthalmol. 126 (2), 227–232.